A Comprehensive Hepatitis C Viral Kinetic Model Explaining Cure

E Snoeck[1], P Chanu[2], M Lavielle[3], P Jacqmin[1], EN Jonsson[1], K Jorga[2], T Goggin[2], J Grippo[2], NL Jumbe[2] and N Frey[2]

We propose a model that characterizes and links the complexity and diversity of clinically observed hepatitis C viral kinetics to sustained virologic response (SVR)—the primary clinical end point of hepatitis C treatment, defined as an undetectable viral load at 24 weeks after completion of treatment)—in patients with chronic hepatitis C (CHC) who have received treatment with peginterferon α-2a ± ribavirin. The new attributes of our hepatitis C viral kinetic model are (i) the implementation of a cure/viral eradication boundary, (ii) employment of all hepatitis C virus (HCV) RNA measurements, including those below the lower limit of quantification (LLOQ), and (iii) implementation of a population modeling approach. The model demonstrated excellent positive (99.3%) and negative (97.1%) predictive values for SVR as well as high sensitivity (96.6%) and specificity (99.4%). The proposed viral kinetic model provides a framework for mechanistic exploration of treatment outcome and permits evaluation of alternative CHC treatment options with the ultimate aim of developing and testing hypotheses for personalizing treatments in this disease.

An estimated 170 million people, or ~2.1% of the world population, are currently infected with hepatitis C virus (HCV); this is more than four times the number of people living with HIV.[1] The current standard of care for patients with chronic hepatitis C (CHC) is the combination of pegylated interferon-α and ribavirin.[2,3] Successful HCV treatment outcome, i.e., sustained virologic response (SVR), is defined as a patient's viral load being below the HCV RNA detection limit at a follow-up evaluation at 24 weeks after the completion of the treatment. In large, randomized, multicenter trials, SVR has been attained in up to 66% of treatment-naive patients by treating with the optimal regimen of peginterferon α-2a plus ribavirin.[4,5] The HCV genotype 1 (G1) virus is more difficult to treat. Patients infected with this genotype—approximately 70% of CHC patients in the United States[6]—are less likely to achieve an SVR as compared with patients infected with HCV non-genotype 1 (Gn1). Approximately 50% of the patients with HCV G1 achieved an SVR when treated with peginterferon α-2a plus ribavirin, whereas ~80% of patients with HCV Gn1 achieved an SVR despite receiving treatment of a shorter duration at a lower dose of ribavirin.[5] Patients with HCV, therefore, represent a population with a continued unmet medical need, with many of them having the potential to attain SVR if optimized treatment approaches are adopted.

The process of modeling HCV dynamics during therapy has led to important insights into the life cycle of the virus, elucidating the kinetic parameters governing viral infection and hepatocyte death, the antiviral effects of interferons, and the manner in which ribavirin affects HCV treatment.[7] Models of HCV kinetics have provided a means to compare varied treatment regimens and outcomes in different patient populations.[8] A model of HCV infection was originally proposed by Neumann *et al.*,[9] who adapted a model of HIV infection.[10,11] The Neumann model adequately describes the typical outcome of short-term therapy, characterized by an initial rapid viral decline followed by a second, slower decline until HCV RNA becomes undetectable.[12,13] This model has been frequently used to describe viral-load profiles after short-term treatment.[8,14,15] However, after the current long-term standard-of-care treatment, the virus is not eradicated in all CHC patients.[5] In the patients who do not attain SVR (i.e., patients in whom the virus is not eradicated), the viral load either rebounds to pretreatment levels during therapy (breakthrough) or returns to pretreatment levels upon cessation of therapy (relapse).[13] The Neumann model cannot describe these two phenomena, and, crucially, it cannot describe SVR.[13] These phenomena are the primary reason that early viral response does not uniformly predict the clinical end point. Finally, and most important, previous analyses have

[1]Exprimo NV, Mechelen, Belgium; [2]F. Hoffmann–La Roche Ltd., Basel, Switzerland; [3]Department of Mathematics, INRIA Saclay, University Paris-Sud, Orsay, France. Correspondence: NL Jumbe (drshasha@gmail.com)

Received 30 October 2009; accepted 13 February 2010; advance online publication 12 May 2010. doi:10.1038/clpt.2010.35

used a naive method of handling the HCV RNA measurements below the lower limit of quantification (LLOQ) by omitting all such data, despite the fact that these contain critical information regarding long-term treatment outcome.

In this article, we propose a novel approach to modeling the viral kinetics in hepatitis C. First, a nonlinear mixed-effects model was developed by maximum likelihood estimation (MLE) of the parameters, using the extended stochastic approximation expectation-maximization (SAEM) algorithm as implemented in the MONOLIX software (http://www.monolix.org). Individual long-term HCV kinetic profiles were simultaneously described for 2,100 patients with CHC who received treatment with peginterferon α-2a, alone or in combination with ribavirin, using a wide spectrum of dosing regimens. Second, HCV RNA measurements below the LLOQ were included. The proposed model permits the distinction between SVR and LLOQ by including censored data residing between the HCV RNA LLOQ and the irrevocable lower boundary of zero. Third, cure or complete virion eradication was determined from viral kinetics via implementation of a viral eradication boundary. At the time point at which treatment drives the system to less than one infected hepatocyte, the production of virions was set to zero. The results from the model, characterizing the differences between patients who attain SVR and those in whom treatment fails, were explored in order to derive hypotheses relating to the mechanisms underlying failure or success of treatment.

RESULTS

The parameters of the model were estimated with good precision (**Table 1**). The typical value of the basic reproduction number R_0 was estimated to be 7.2, with an interindividual variability of 137% coefficient of variation. The relatively large interindividual variability probably reflects the large intrinsic biological differences in CHC disease. R_0 represents the relative drug-effect distance from the treatment intervention goal, the goal being to drive the reproduction number during treatment (R_T) to <1 (**Supplementary Note S2** online), so as to increase the likelihood of attaining SVR (i.e., cure, defined as I <1 infected hepatocyte). Indeed, inspection of the individual parameter estimates in patients experiencing a breakthrough during therapy showed that the administered drug therapy failed to decrease the reproduction number (R_T) to <1.[16,17] The maximum hepatocyte proliferation rate (r) was 0.00562/day, and simulations based on this value of r revealed, in 51 liver graft donors, that predicted extent of liver regeneration matched well with the observed increases in liver volumes as measured at 1 year after the right-lobe liver graft donation (relative to the respective volumes immediately after the surgery) (**Supplementary Note S3** online[18]). The typical value of the virion production rate P was 25.1 virions/day, and the free virion clearance rate c was estimated to be 4.53/day, corresponding to a free virion half-life of 3.7 h. This half-life lies within the previously reported range of 1.5–4.6 h.[12,13] The free virion clearance rate was found not to be influenced by HCV genotype. In contrast, the infected cell death rate (δ) appeared to

Table 1 Population parameters of the HCV viral kinetic model fitted to the individual long-term viral-load profiles of 2,100 patients with CHC receiving chronic treatment with peginterferon α-2a, alone or in combination with ribavirin[a]

Parameter	Description	Unit	Typical value	SE (% CV)[c]	IIV (% CV)
T_{max}	Total number of hepatocytes per ml	Hepatocytes/ml	18.5×10^6		
s	Hepatocyte production rate	Hepatocytes/ml/day	61.7×10^3		
D	Hepatocyte death rate constant	Per day	0.003		
r	Hepatocyte proliferation rate constant	Per day	0.00562	22	
R_0[d]	Basic reproductive number		7.15	9	137
p	Virion production rate	Virions·hepatocyte/day	25.1	15	
c	Virion elimination rate constant	Per day	4.53	15	120
$\delta_{HCV\ non\text{-}1}$	Infected cell death rate constant (HCVGn1)	Per day	0.192	16	58[b]
$\delta_{HCV\text{-}1}$	Infected cell death rate constant (HCV G1)	Per day	0.139	3	58[b]
$ED_{50_{PEG}HCVnon\text{-}1}$	ED_{50} of peginterferon α-2a (HCV Gn1)	μg/week	1.19	17	281[b]
$ED_{50_{PEG}HCV\text{-}1}$	ED_{50} of peginterferon α-2a (HCV G1)	μg/week	20.9	10	281[b]
$ED_{50_{RBV}}$	ED_{50} of ribavirin	mg/kg/day	14.4	18	
K	Antiviral-effect decay constant	Per day	0.0238	13	
σ^2	Residual error		0.260	1	

The upper part of the table shows the fixed parameters according to our assumptions, the middle of the table shows system-specific parameters, and the lower part shows the drug-specific parameters. The SE reflects the precision of the estimated parameters, and IIV represents the interindividual variability (**Supplementary Note S5** online).

CHC, chronic hepatitis C; CV, coefficient of variation; G1, genotype 1; Gn1, non-genotype 1; HCV, hepatitis C virus.

[a]47% received monotherapy with peginterferon α-2a at a weekly subcutaneous dose of 45 μg (20 patients), 90 μg (114 patients), 135 μg (210 patients), 180 μg (596 patients), or 270 μg (38 patients). The patients with CHC and combination therapy were administered a subcutaneous dose of 180 μg/week of peginterferon α-2a and a daily dose of 800 mg or 1,000/1,200 mg of ribavirin. Almost all patients (93%) received 24 weeks of treatment or more, and 61% of patients received 48 weeks of treatment or more. [b]Assumed to be similar between patients with HCV genotype 1 and non–genotype 1 infections. [c]Because T_{max}, s, and d were fixed, no SE is provided. [d]R_0 is defined as the number of newly infected cells that arise from one infected cell when almost all cells are uninfected, and therefore has no units.

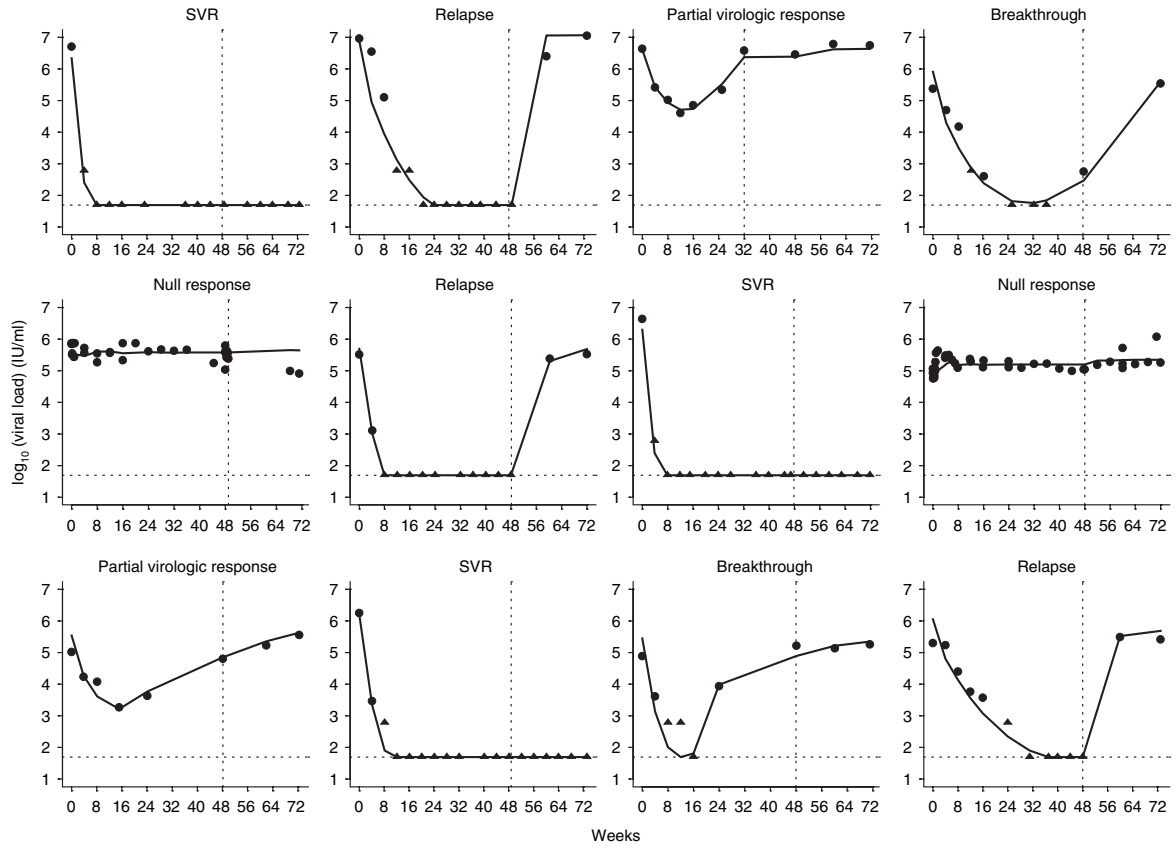

Figure 1 Observed and model-predicted long-term viral-load profiles in 12 representative patients with CHC. Solid lines are the fits of the model to the individual viral-load data which are either detectable (closed circles) or below the LLOQ of 50 IU/ml (closed triangles). Dotted horizontal lines show the LLOQ of the assay. Dotted vertical lines indicate the end of treatment. Our HCV viral kinetic model is able to describe all the typical phenomena observed after long-term therapy, such as null response (no change in viral load), partial virologic response (initial decrease followed by increase during treatment), breakthrough during therapy (undetectable viral load followed by increase during treatment), relapse after therapy (undetectable viral load at the end of therapy followed by an increase during the treatment-free follow-up period), and SVR (undetectable viral load at 24 weeks after end of therapy). CHC, chronic hepatitis C; HCV, hepatitis C virus; LLOQ, lower limit of quantification; SVR, sustained virologic response.

be dependent on HCV genotype, and the typical value was estimated to be 0.139/day in patients with HCV G1 infection and 0.192/day in patients infected with HCV Gn1 (**Table 1**). These estimates are in line with previously reported values of δ.[19] The higher δ in patients with HCV Gn1 may indicate an enhanced immunological response and is in line with the previous finding that a fast viral decay early in treatment correlates with an enhanced tendency to attain SVR.[19] Also, the typical value of the $ED_{50_{PEG}}$ was found to be lower in patients with HCV Gn1 as compared with patients infected with HCV G1, thereby confirming the higher effectiveness of peginterferon α-2a in blocking virion production in Gn1 patients (**Table 1** and ref. 20,21). The $ED_{50_{RBV}}$ was estimated to be 14.4 mg/kg/day, which is equivalent to rendering 40–60% of the virions noninfectious on a standard ribavirin treatment of 1,000/1,200 mg/day (see Equation 6). The antiviral-effect decay constant (K) was estimated to be 0.0238/day, which corresponds to a half-life of ~29 days. Given that the terminal half-life after multiple dosing with peginterferon α-2a is ~160 h and that of ribavirin is ~12 days,[20,21] the antiviral effect decay constant may describe both pharmacokinetic and pharmacodynamic processes. Finally, the variance in the residual error (σ^2) was estimated to be 0.260. The residual error is relatively high, but this is not uncommon for viral kinetic models; for instance, a σ^2 value of 0.38 was obtained previously in a similar analysis of HIV viral-load data.[22]

Model evaluation and qualification

The goodness-of-fit assessment revealed that the individual viral-load profiles are well described by the model (**Supplementary Note S4** online). Population-based diagnostics were also used, but they are not easily interpretable unless simulated reference graphs from the true model are used for comparison (**Supplementary Note S4** online[23]). A selection of 12 individual viral-load profiles shows that the HCV viral kinetic model is able to describe not only the initial decreases in viral load over the first month but also the typical phenomena observed after longer-term therapy (**Figure 1**). The model provided satisfactory positive (99.3%) and negative (97.1%) predictive values for SVR, along with high sensitivity (96.6%) and specificity (99.4%) (**Supplementary Note S5** online).

The predictive performance of the model was assessed by a model-evaluation procedure using the design and data of a large clinical trial not included in the model-building data set.[4] The model was successfully qualified for further simulations, given

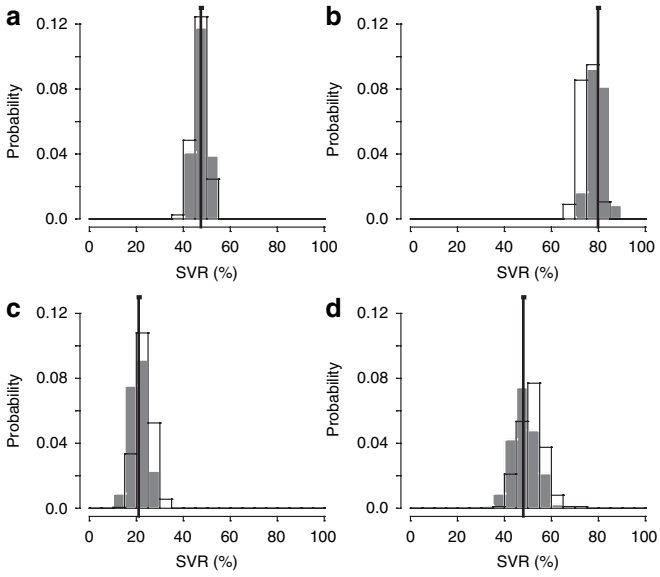

Figure 2 Observed (black vertical lines) and model-predicted SVR data (transparent histogram) of the phase III study by Fried *et al.*[4] investigating the effect of 180 µg of peginterferon α-2a once weekly for 48 weeks, given alone or in combination with a daily dose of 1,000 or 1,200 mg of ribavirin. Dropouts have been taken into account in the predictions by randomly assigning patients as dropouts and defining them as non-SVR. The uncertainty of the observed SVR percentages was quantified by 400 bootstrap samples (gray histograms). (**a**) The observed SVR outcomes in 297 HCV G1 patients receiving combination therapy fall within the range of model-predicted SVR outcomes. (**b**) The observed SVR outcomes in 154 HCV Gn1 patients receiving combination therapy also fall within the range of model-predicted outcomes. (**c**) The observed SVR outcomes in 143 patients with HCV G1 receiving monotherapy with peginterferon α-2a fall within the range of model-predicted SVR outcomes. (**d**) Finally, the observed SVR outcomes in 77 patients with HCV Gn1 receiving monotherapy with peginterferon α-2a fall within the range of model-predicted SVR outcomes. G1, genotype 1; Gn1, non-genotype 1; HCV, hepatitis C virus; SVR, sustained virologic response.

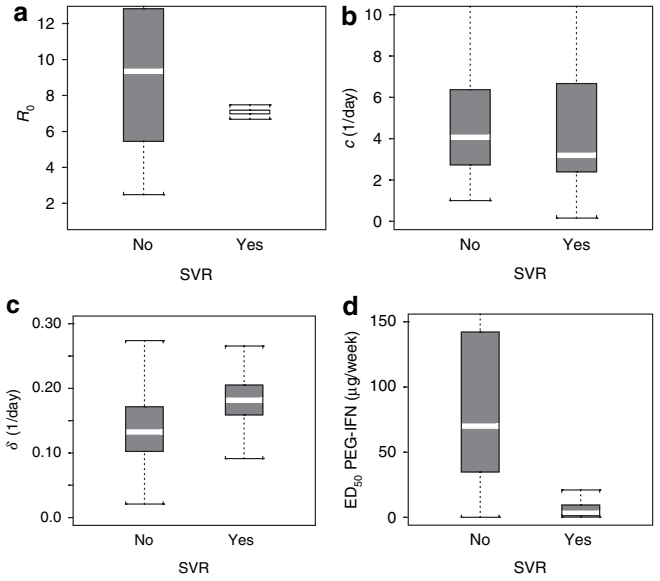

Figure 3 Box plots of the individual HCV viral kinetic model parameters as categorized by patient outcome (i.e., SVR (n = 974) vs. non-SVR (n = 1,126) patients). (**a**) The basic reproduction number (R_0) is generally higher and more variable in patients who do not attain SVR. (**b**) The free virion clearance rate (c) is not different between patients who attain SVR and those who do not. (**c**) The infected-cell death rate (δ) is generally higher in patients who attain SVR, and (**d**) the effectiveness of peginterferon α-2a (PEG-IFN) in inhibiting the production of new virions is generally higher in patients who attain SVR. HCV, hepatitis C virus; SVR, sustained virologic response.

the fact that the predicted range of SVR-attainment percentages in patients with HCV G1 and Gn1 infections receiving 48 weeks of treatment with peginterferon α-2a, alone or in combination with ribavirin, matched well with the observed values in this study (**Figure 2**).

DISCUSSION

The multidimensional interactions between HCV virus, host, and drug are highly nonlinear, and equilibrium outcomes quickly become counterintuitive.[24] Here, we propose a population approach using MLE by the extended SAEM algorithm as implemented in the MONOLIX software (http://www.monolix.org), in order to simultaneously describe individual long-term HCV kinetic profiles of 2,100 CHC patients treated with peginterferon α-2a, alone or in combination with ribavirin. The four ordinary differential equations of the HCV viral kinetic model (Equations 1–4) were implemented in MONOLIX. HCV viral kinetic models encompassing ordinary differential equations have previously been used for exploratory simulations;[17,25] however, they have not been used for simultaneously fitting the complexity and diversity of clinically observed HCV viral kinetics.

The proposed model addresses the host–virus–drug interactions by advancing both previously known and novel ideas from a population perspective, simultaneously analyzing a wide spectrum of treatment regimens (drug combinations, doses, and schedules as well as treatment durations), incorporating left-censored data previously largely excluded from analysis, and implementing a viral-eradication cure boundary to link viral kinetics to clinical outcome (i.e., SVR). The final viral kinetic model was qualified using internal and external data sets, including those from patients with HCV G1 and Gn1 infections, and it demonstrated positive and negative predictive values as well as sensitivity and specificity exceeding 96%.

In clinical practice, milestone target treatment strategies—that is, rapid virologic response, defined as attainment of undetectable HCV RNA levels by week 4 of therapy,[3,26] and early virologic response, defined as attainment of a ≥2 log reduction or undetectable levels of serum HCV RNA at week 12 of treatment—have been proposed for the optimization of SVR percentages by modifying treatment duration. However, these early treatment-response landmarks (regardless of time point) do not uniformly predict SVR because there is the potential for viral load either to rebound to pretreatment levels during therapy (breakthrough) or to return to pretreatment levels upon cessation of therapy (relapse). This observation leads to two conclusions: (i) the relationship between rapid virologic response/early virologic response and SVR is correlative but not prescriptive and (ii) exclusion of HCV RNA measurements below the LLOQ (i.e., left-censoring) probably biases SVR predictions. An extension

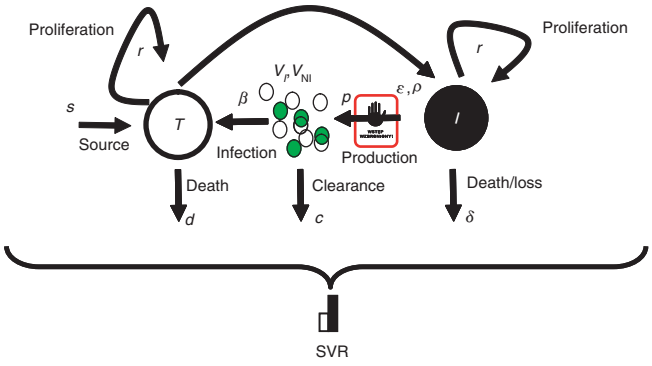

Figure 4 Representation of the extended HCV viral kinetic model. Infectious HCV virions (V_I) infect target cells (T), creating productively infected hepatocytes (I). Uninfected hepatocytes (T) are produced at rate s and die at rate d. Infected hepatocytes die at rate δ. A density-dependent proliferation of hepatocytes (r) is assumed. Infectious (V_I) and noninfectious (V_{NI}) virions are produced at rate p and cleared at rate c. Peginterferon α-2a dose-dependently inhibits the production of new virions (ε), and ribavirin dose-dependently renders a fraction of newly produced virions noninfectious (ρ). SVR, defined as the status of having an undetectable viral load at 24 weeks after completion of treatment, is the primary clinical end point desired to be predicted in the treatment of hepatitis C. HCV, hepatitis C virus; SVR, sustained virologic response.

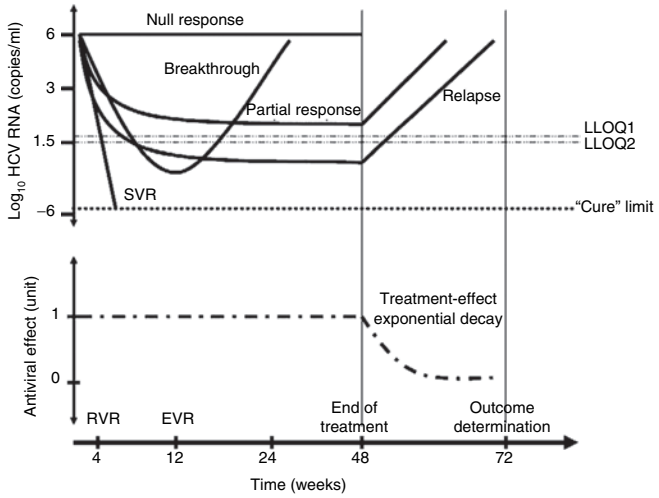

Figure 5 The viral kinetic model characterizes the complexity and diversity of clinically observed HCV viral kinetics in patients with hepatitis C virus infection treated with peginterferon α-2a, alone or in combination with ribavirin, and links the kinetics to clinical outcome. This is achieved by the implementation of a viral-eradication cure boundary and incorporation of left-censored data, largely excluded from analysis in earlier studies, in a simultaneous analysis of a wide spectrum of peginterferon α-2a ± ribavirin treatment regimens in 2,100 patients. EVR, early virologic response; HCV, hepatitis C virus; LLOQ, lower limit of quantification; RVR, rapid virologic response.

of the SAEM algorithm as implemented in the MONOLIX software handles left-censored data in nonlinear mixed-effects models with computational efficiency.[22] A comparison with classic methods of handling missing data shows that the extended SAEM algorithm is less biased than the exclusion of data related to subjects with censored measurements, omission of all censored data points, and/or imputation to half the quantification limit for the first point below the LLOQ with omission of the subsequent missing data.[27] Furthermore, the extended SAEM algorithm has been demonstrated to be more efficient and/or less biased than linearization or Monte Carlo approximation of the expectation step applied to censored values.[22]

The implementation of the cure boundary in the viral kinetic model is based on physiological considerations and is consistent with the primary goal of HCV therapy, which is to completely eradicate the virus. The final viral kinetic model was implemented as a two-state system. The off state (null virion production) is triggered when there is less than one infected hepatocyte in the total plasma and extracellular fluid volume of distribution, thereby resulting in cure/SVR. The on state (constitutive virion production) returns the patient to full-blown disease when even only a minute fraction of one infected hepatocyte remains.

A comparison of the individual parameter estimates for patients who attain SVR with those for patients who do not reveals that R_0 and $ED_{50_{PEG}}$ are generally lower in patients who attain SVR (**Figure 3**). A relatively low R_0 prior to treatment and a relatively high inhibition of virion production increase the likelihood of $R_T < 1$ during treatment and will therefore increase the likelihood of SVR.

Indeed, inspection of the individual parameter estimates in patients experiencing a breakthrough during therapy showed that the administered drug therapy failed to decrease the R_T to <1.[16,17] According to our modeling assumptions, a treatment with either higher doses or a combination treatment with new drugs may be an option in these patients in order to drive R_T to <1. Possible explanations for relapse at the end of the treatment period are (i) the patients may have reached an $R_T < 1$ during treatment but were not treated long enough to cross the cure boundary of I < 1 cell, such that the viral load quickly returned to its original numbers at the end of therapy, or (ii) drug therapy may have failed to decrease the R_T to <1 (inadequate efficacy). The extension of treatment duration at the same drug combination, dose, and schedule may therefore be an option for patients in the former category but not for those in the latter. On the basis of these hypotheses, individual treatments may be optimized when the individual R_0 and inhibition of the virion production are predetermined or determined early after the onset of treatment. The relationship between treatment duration, dose and schedule, and/or likelihood of crossing the cure boundary after high-dose induction has yet to be fully elucidated.

In our model-based analysis, the free virion clearance rate (c) did not appear to be a prognostic factor for SVR (**Figure 3**), whereas the death rate of infected cells (δ) was found to be generally higher in patients who went on to attain SVR. This would indicate that these patients may have an enhanced immunological response and therefore a higher likelihood of attaining viral eradication.

Our proposed viral kinetic model is a simplification of the complex interaction between host, infected hepatocytes, virus, and mechanisms of drug action; it required the fixing of several liver physiology parameters to biologically justifiable values, as explained below. Furthermore, the combination of peginterferon

α-2a and ribavirin is assumed to inhibit the virion production (p) in a multiplicative manner, in accordance with E_{max} dose–response relationships. Although some confidence in the predictive performance of the model is derived from the qualification exercise described above, a complete understanding of the implications of these assumptions has not been achieved, and they should be further explored—particularly with respect to use of the model to explore the efficacy of new drugs in combination with standard of care. Another limitation of this model is the fact that dose was used as the perturbation to the system. Given that HCV standard-of-care pharmacotherapy has been established through empirical study over a decade, investigation of schedule dependence was not considered to be primary to our objectives. This implies that a pharmacokinetics model component will need to be added to the current model for evaluating schedule dependence and/or adherence, especially for the drugs with shorter pharmacokinetic half-lives that are being developed.

In summary, our population HCV viral kinetic model was able to adequately describe all individual long-term viral-load profiles of 2,100 CHC patients receiving chronic treatment with peginterferon α-2a, alone or in combination with ribavirin. The model provides new insights and explanations for typical phenomena observed in the clinic, such as breakthrough during therapy, relapse after stopping therapy, and cure (or SVR). Simulations based on our model may help to improve our understanding of current treatment success and failure, and they can also be used to predict and evaluate the efficacy of alternative treatment options (e.g., alternative doses, durations, and, with additional assumptions worked into the model, new drug combinations) in the overall population of CHC patients. These will be described in a follow-up communication. The proposed viral kinetic model provides a framework for developing and testing hypotheses for evaluating new antiviral agents and personalizing treatments for CHC that would ultimately need to be validated in well-designed clinical trials.

METHODS

Patients and data. Data from one phase II study and four phase III studies of peginterferon α-2a (40 kDa) (Pegasys, Genentech, South San Francisco, CA, USA), alone or in combination with ribavirin (Copegus, Roche Laboratories, Nutley, NJ, USA), were pooled. All the patients were required to have histologically and serologically proven CHC. The complete inclusion and exclusion criteria, study design, and primary results have been published elsewhere.[5,28–31] A total of 2,100 patients with CHC were included in the final database. Serum HCV RNA (COBAS AMPLICOR HCV Test, version 2.0; Roche Molecular Diagnostics, Pleasanton, CA) was measured at specific time points during treatment and over the 24-week untreated follow-up period. All the 21,284 HCV RNA measurements available, of which 59% were below the LLOQ, were modeled by accounting for the left-censoring in the analysis. The LLOQs of the two assays used were 50 IU/ml and 600 IU/ml, respectively.[32]

HCV viral kinetic model. The viral kinetic model (Equations 1–4) extends the original Neumann[9] model to include important contributions by Dahari *et al.* (density-dependent proliferation of hepatocytes (r)[16]) and Pomfret *et al.* (hepatocyte intrinsic production[18]). The treatment effect of peginterferon α-2a (ε) and the effect of ribavirin rendering a fraction of newly produced virions noninfectious (ρ)[7] directly impacted the virion production rate (p). The model structure of the viral kinetic model (**Figure 4**) is described by the following mass balance equations:

$$\frac{dT}{dt} = s + r \cdot T \cdot \left(1 - \frac{T+I}{T_{max}}\right) - d \cdot T - \beta \cdot V_I \cdot T \quad (1)$$

$$\frac{dI}{dt} = \beta \cdot V_I \cdot T + r \cdot I \cdot \left(1 - \frac{T+I}{T_{max}}\right) - \delta \cdot I \quad (2)$$

$$\frac{dV_I}{dt} = (1-\rho)\cdot(1-\varepsilon)\cdot p \cdot I - c \cdot V_I \quad (3)$$

$$\frac{dV_{NI}}{dt} = \rho \cdot (1-\varepsilon) \cdot p \cdot I - c \cdot V_{NI} \quad (4)$$

where infectious HCV virions (V_I) infect target cells (uninfected hepatocytes) (T), creating productively infected cells (I) at a rate $\beta \cdot V_I \cdot T$. Uninfected hepatocytes are produced at rate s and die at rate d. Infected hepatocytes die at rate δ. As in the study by Dixit *et al.*,[7] it is assumed that infectious (V_I) and noninfectious (V_{NI}) virions are produced from infected hepatocytes at rate p and cleared at rate c. The measured viral load (V) is expressed in IU/ml, representing the sum of infectious and noninfectious virions: $V = V_I + V_{NI}$. The model was further extended with E_{max} dose–response models describing the dose-dependent effects of peginterferon α-2a and ribavirin:

$$\varepsilon = \frac{\text{Dose}_{PEG}}{\text{ED}_{50_{PEG}} + \text{Dose}_{PEG}} \quad (5)$$

$$\rho = \frac{\text{Dose}_{RBV}}{\text{ED}_{50_{RBV}} + \text{Dose}_{RBV}} \quad (6)$$

where Dose_{PEG} is the weekly subcutaneous dose of peginterferon α-2a and $\text{ED}_{50_{PEG}}$ is the estimated weekly dose of peginterferon α-2a that results in a 50% inhibition of the virion production. Similarly, Dose_{RBV} is the daily dose of ribavirin/kg body weight, and $\text{ED}_{50_{RBV}}$ is the estimated daily dose in mg/kg that renders 50% of the virions noninfectious. Dose_{RBV} and $\text{ED}_{50_{RBV}}$ were expressed as mg/kg because ribavirin is dosed by body weight and ribavirin expressed in mg/kg has previously been found to be a prognostic factor for SVR.[33]

The implementation of a cure/virus-eradication boundary represents a milestone contribution to the linking of the complexity and diversity of clinically observed hepatitis C viral kinetics to SVR. The cure boundary was based on the assumption that virion production (p) should cease when all infected cells are cleared, i.e., when there is less than one infected cell in the total plasma and extracellular fluid volume of ~13.5×10^3 ml. At the time point at which the antiviral effect of the treatment drove the system to a status of less than one infected hepatocyte, the virion production p was set to zero (the off state), resulting in a model cure/SVR (**Supplementary Note S1** online). Exploratory simulations without this additional model component of cure predicted rapid viral-load return to original numbers in all CHC patients when treatment was stopped (**Supplementary Note S1** online), whereas in reality the virus is eradicated after the current standard treatment of care in the majority of patients with HCV Gn1 infection and in ~50% of those with HCV G1 infection.[5]

A fundamental parameter of the viral kinetic model is the estimated basic reproduction number (R_0) (**Supplementary Note S2** online[17]). It was previously shown that the reproduction number in the presence of an inhibitor (R_T) is given by:

$$R_T = R_0 \cdot (1 - \varepsilon_T) \quad (7)$$

where ε_T is the total treatment-induced inhibition of the virion production (P. Jacqmin, E. Snoeck, and E.N. Jonsson, unpublished data). Because

infection in the presence of an inhibitor has been shown to be cleared when $R_T < 1$ (P. Jacqmin *et al.*, unpublished data), ε_T combined with R_0 is an important predictor for a successful drug therapy. For this reason, our model was parameterized in terms of R_0, using the following equation for R_0:[17]

$$R_0 = \frac{p \cdot \beta \cdot s}{c \cdot \delta \cdot d} \quad (8)$$

Finally, drug effect after stopping treatment was described by an exponential decay function ($e^{-K \cdot t}$, **Figure 5**), where K is the estimated antiviral-effect decay constant and t the time from the end of treatment. Without the inclusion of this exponential decay function, the predicted viral load in patients whose disease relapsed after stopping therapy appeared to return too rapidly to pretreatment values.

Assumptions in the model. Currently available data did not allow the estimation of all parameters of the declared viral kinetic model owing to issues of mathematical identifiability. For this reason, a number of system/physiological parameters were fixed to biologically justifiable values. The maximum number of hepatocytes present in an individual liver was assumed to be 2.50×10^{11} (ref. 34). Because HCV RNA is distributed in plasma and extracellular fluids with a volume of $\sim 13.5 \times 10^3$ ml,[35] the maximum number of hepatocytes (T_{max}) was assumed to be 18.5×10^6 cells/ml.[12] Assuming that in a healthy liver there is hepatocyte turnover every 300 days,[36] the death rate of target cells (d) was set to 1/300/day, and therefrom ($T_{max} \cdot d$) the production of new hepatocytes in the absence of liver disease (s) could be assumed to be 61.7×10^3 cells/ml/day.[12] Estimated proliferation rates were set to be equal across infected and uninfected hepatocytes, given the absence of any direct information to the contrary.

Nonlinear mixed-effects models comprise a combination of fixed and random effects. Individual parameters (PAR_i) in such a model are assumed to be log-normally distributed and can be described by:

$$PAR_i = \theta \cdot e^{\eta_i} \quad (9)$$

where the subscript i denotes individual, the fixed-effects parameter θ represents the median (typical) value of the parameter in the population, and η_i is the random effect accounting for the individual difference from the typical value. The η_i values are assumed to be normally distributed in the population, with a mean of zero and an estimated variance of ω^2. Individual parameter estimates are used to predict the viral load in an individual i at a certain point in time j ($V_{pred,ij}$). The measured viral-load data ($V_{obs,ij}$) were $\log_{10}$-transformed for the analysis so as to enable handling of the wide range of viral-load observations, and an additive residual-error model was used for the $\log_{10}$-transfomed viral-load data:

$$\log_{10} V_{obs,ij} = \log_{10} V_{pred,ij} + \varepsilon_{ij} \quad (10)$$

The ε_{ij} values are assumed to be normally distributed with a mean of zero and an estimated variance of σ^2. The ω^2 value quantifies the interindividual variability, and the σ^2 value quantifies the residual variability.

Estimated fixed-effects parameters were R_0, p, c, δ, liver proliferation rate r (**Supplementary Note S3** online[16]), $ED_{50_{PEG}}$, $ED_{50_{RBV}}$, and K. Interindividual variability was incorporated on the parameters R_0, c, δ, and $ED_{50_{PEG}}$.

Parameter estimation. Population parameters of our HCV viral kinetic model were estimated using MLE by the SAEM algorithm for hierarchical nonlinear mixed-effects model analysis.[37,38] Individual parameters were obtained by computing for each patient the so-called maximum *a posteriori* estimate, which maximizes the conditional distribution of the individual parameters using the MLE of the population parameters computed previously with the SAEM algorithm.[38] SAEM is a powerful algorithm for MLE in complex models, including dynamic models defined by a system of ordinary differential equations. Furthermore, the left-censored data are properly handled by the extended SAEM algorithm for MLE as described by Samson *et al.*[22] The extended SAEM algorithm for MLE is implemented in the MONOLIX software, available on the author's website (http://www.monolix.org). We used version 2.4.

Evaluation and qualification of the model. Goodness of fit was assessed by the method of simulating from the final model and refitting.[23] Because, by definition, the proposed model does not characterize SVR directly, and SVR is derived from crossing the model cure boundary, the predictive performance of the model in correctly classifying patients into SVR or non-SVR categories, which is considered one of the core utilities of the model, could be assessed by calculating the sensitivity and specificity[39,40] without confounding bias. The predictive performance of the model was assessed by a model-evaluation procedure using the design and data of a large clinical trial not included in the model-building data set. In this trial, 180 µg peginterferon α-2a was administered once weekly for 48 weeks, alone or in combination with a daily dose of 1,000 or 1,200 mg ribavirin.[4] Dropout rates in the simulated cohort were matched to historical data by random assignment, and dropouts were defined as non-SVR. The uncertainty of the observed percentages of SVR was quantified by 400 bootstrap samples and compared with observed SVR data in the trial.

ACKNOWLEDGMENTS

We wish to pay tribute to the 2,100 patients whose data are included in this analysis, the physicians and nurses who took care of them, and the Pegasys Life Cycle Team for their vision and support in the development of this model. We thank Frank Duff, Annabelle Lemenuel, and Rohit Kulkarni for their scientific input and editorial assistance and Sharon Lim and Marlene Hering for their help in the preparation of this manuscript.

CONFLICT OF INTEREST

P.C., K.J., T.G., J.G., N.L.J., and N.F. are employees of F. Hoffmann–La Roche Ltd. E.S., P.J., and E.N.J. are compensated F. Hoffmann–La Roche consultants. M.L. is the developer of MONOLIX and declared no conflict of interest.

© 2010 American Society for Clinical Pharmacology and Therapeutics

1. World Health Organization. Hepatitis C <http://www.who.int/mediacentre/factsheets/fs164/en>. Accessed 15 September 2008.
2. National Institutes of Health. National Institutes of Health Consensus Development Conference Statement: management of hepatitis C: 2002—June 10–12, 2002. *Hepatology* **36**, S3–S20 (2002).
3. Strader, D.B., Wright, T., Thomas, D.L. & Seeff, L.B.; American Association for the Study of Liver Diseases. Diagnosis, management, and treatment of hepatitis C. *Hepatology* **39**, 1147–1171 (2004).
4. Fried, M.W. *et al*. Peginterferon alfa-2a plus ribavirin for chronic hepatitis C virus infection. *N. Engl. J. Med*. **347**, 975–982 (2002).
5. Hadziyannis, S.J. *et al*.; PEGASYS International Study Group. Peginterferon-alpha2a and ribavirin combination therapy in chronic hepatitis C: a randomized study of treatment duration and ribavirin dose. *Ann. Intern. Med*. **140**, 346–355 (2004).
6. Zein, N.N., Rakela, J., Krawitt, E.L., Reddy, K.R., Tominaga, T. & Persing, D.H. Hepatitis C virus genotypes in the United States: epidemiology, pathogenicity, and response to interferon therapy. Collaborative Study Group. *Ann. Intern. Med*. **125**, 634–639 (1996).
7. Dixit, N.M., Layden-Almer, J.E., Layden, T.J. & Perelson, A.S. Modelling how ribavirin improves interferon response rates in hepatitis C virus infection. *Nature* **432**, 922–924 (2004).
8. Perelson, A.S., Herrmann, E., Micol, F. & Zeuzem, S. New kinetic models for the hepatitis C virus. *Hepatology* **42**, 749–754 (2005).
9. Neumann, A.U. *et al*. Hepatitis C viral dynamics *in vivo* and the antiviral efficacy of interferon-alpha therapy. *Science* **282**, 103–107 (1998).
10. Perelson, A.S., Neumann, A.U., Markowitz, M., Leonard, J.M. & Ho, D.D. HIV-1 dynamics *in vivo*: virion clearance rate, infected cell life-span, and viral generation time. *Science* **271**, 1582–1586 (1996).
11. Wei, X. *et al*. Viral dynamics in human immunodeficiency virus type 1 infection. *Nature* **373**, 117–122 (1995).
12. Colombatto, P. *et al*. Sustained response to interferon-ribavirin combination therapy predicted by a model of hepatitis C virus dynamics using both HCV RNA and alanine aminotransferase. *Antivir. Ther. (Lond.)* **8**, 519–530 (2003).

13. Zeuzem, S. The kinetics of hepatitis C virus infection. *Clin. Liver Dis*. **5**, 917–930 (2001).
14. Layden, J.E. & Layden, T.J. Viral kinetics of hepatitis C: new insights and remaining limitations. *Hepatology* **35**, 967–970 (2002).
15. Layden-Almer, J.E., Cotler, S.J. & Layden, T.J. Viral kinetics in the treatment of chronic hepatitis C. *J. Viral Hepat*. **13**, 499–504 (2006).
16. Dahari, H., Lo, A., Ribeiro, R.M. & Perelson, A.S. Modeling hepatitis C virus dynamics: liver regeneration and critical drug efficacy. *J. Theor. Biol*. **247**, 371–381 (2007).
17. Callaway, D.S. & Perelson, A.S. HIV-1 infection and low steady state viral loads. *Bull. Math. Biol*. **64**, 29–64 (2002).
18. Pomfret, E.A. *et al*. Liver regeneration and surgical outcome in donors of right-lobe liver grafts. *Transplantation* **76**, 5–10 (2003).
19. Neumann, A.U. *et al*. Differences in viral dynamics between genotypes 1 and 2 of hepatitis C virus. *J. Infect. Dis*. **182**, 28–35 (2000).
20. US Food and Drug Administration. Label information for Pegasys <http://www.fda.gov/downloads/Drugs/DrugSafety/ucm088679.pdf>.
21. US Food and Drug Administration. Label information for Copegus <http://www.fda.gov/downloads/Drugs/DrugSafety/ucm088576.pdf>.
22. Samson, A., Lavielle, M. & Mentré, F. Extension of the SAEM algorithm to left-censored data in nonlinear mixed-effects model: Application to HIV dynamics model. *Comput. Statist. Data Anal*. **51**, 1562–1574 (2006).
23. Karlsson, M.O. & Savic, R.M. Diagnosing model diagnostics. *Clin. Pharmacol. Ther*. **82**, 17–20 (2007).
24. Bernardin, F., Tobler, L., Walsh, I., Williams, J.D., Busch, M. & Delwart, E. Clearance of hepatitis C virus RNA from the peripheral blood mononuclear cells of blood donors who spontaneously or therapeutically control their plasma viremia. *Hepatology* **47**, 1446–1452 (2008).
25. Wodarz, D. Mathematical models of immune effector responses to viral infections: virus control versus the development of pathology. *J. Comp. Appl. Math*. **184**, 301–319 (2005).
26. Dienstag, J.L. & McHutchison, J.G. American Gastroenterological Association technical review on the management of hepatitis C. *Gastroenterology* **130**, 231–64; quiz 214 (2006).
27. Samson, A., Lavielle, M. & Mentré, F. The SAEM algorithm for group comparison tests in longitudinal data analysis based on non-linear mixed-effects model. *Stat. Med*. **26**, 4860–4875 (2007).
28. Heathcote, E.J. *et al*. Peginterferon α-2a in patients with chronic hepatitis C and cirrhosis. *N. Engl. J. Med*. **343**, 1673–1680 (2000).
29. Zeuzem, S. *et al*. Peginterferon α-2a in patients with chronic hepatitis C. *N. Engl. J. Med*. **357**, 124–134 (2007).
30. Reddy, K.R. *et al*. Efficacy and safety of pegylated (40-kd) interferon alpha-2a compared with interferon alpha-2a in noncirrhotic patients with chronic hepatitis C. *Hepatology* **33**, 433–438 (2001).
31. Pockros, P.J. *et al*.; PEGASYS International Study Group. Efficacy and safety of two-dose regimens of peginterferon alpha-2a compared with interferon alpha-2a in chronic hepatitis C: a multicenter, randomized controlled trial. *Am. J. Gastroenterol*. **99**, 1298–1305 (2004).
32. Lee, S.C. *et al*. Improved version 2.0 qualitative and quantitative AMPLICOR reverse transcription-PCR tests for hepatitis C virus RNA: calibration to international units, enhanced genotype reactivity, and performance characteristics. *J. Clin. Microbiol*. **38**, 4171–4179 (2000).
33. Snoeck, E., Wade, J.R., Duff, F., Lamb, M. & Jorga, K. Predicting sustained virological response and anaemia in chronic hepatitis C patients treated with peginterferon α-2a (40KD) plus ribavirin. *Br. J. Clin. Pharmacol*. **62**, 699–709 (2006).
34. Sherlock, S. & Dooley, J. *Diseases of the Liver and Biliary System* 10th edn. (Blackwell Science, Oxford, UK, 1998) 8.
35. Liou, T.C., Chang, T.T., Young, K.C., Lin, X.Z., Lin, C.Y. & Wu, H.L. Detection of HCV RNA in saliva, urine, seminal fluid, and ascites. *J. Med. Virol*. **37**, 197–202 (1992).
36. Mc Sween, R.N.M., Anthony, P.P. & Scheuer, P.J. *Pathology of the Liver* 2nd edn. (Churchill-Livingstone, New York, 1987).
37. Delyon, B., Lavielle, M. & Moulines, E. Covergence of a stochastic approximation version of the EM algorithm. *Ann. Statist*. **27**, 94–128 (1999).
38. Kuhn, E. & Laveille, M. Maximum likelihood estimation in nonlinear mixed effects models. *Comput. Statist. Data Anal*. 1020–1038 (2005).
39. Altman, D.G. & Bland, J.M. Diagnostic tests. 1: Sensitivity and specificity. *BMJ* **308**, 1552 (1994).
40. Bishop, Y.M., Fienberg, S.E. & Holland, P.W. *Discrete Multivariate Analysis: Theory and Practice* (MIT Press, Cambridge, MA, 1977).